Preclinical Characterization and In Vivo Imaging Studies of an Engineered Recombinant Technetium-99m-Labeled Metallothionein-Containing Anti-Carcinoembryonic Antigen Single-Chain Antibody

Geoffrey A. Pietersz, Mark R. Patrick and Kerry A. Chester

Austin Research Institute, Austin Hospital, Heidelberg, Victoria, Australia; and Royal Free Hospital School of Medicine, London, United Kingdom

We describe the engineering of a novel single-chain fragment (scFv) metallothionein (MET) containing anti-carcinoembryonic antigen (CEA) antibody (referred to as MET-scFv) for use as a diagnostic imaging agent in colorectal cancer. **Methods:** Site-directed cloning of annealed oligonucleotides, containing both the MET and a c-*myc* tag sequence, into a pUC19-based expression vector enabled soluble secreted protein expression from *Escherichia coli*. Affinity purification was used to purify the protein using an anti-c-*myc* affinity column. The specificity of both the unlabeled and labeled MET-scFv for CEA was demonstrated by solid-phase enzyme-linked immunosorbent assay and radioimmunoassay and by fluorescence-activated cell sorting analysis on CEA-expressing human colorectal LS-174T cells. Technetium-99m labeling was achieved using a Zn^{2+} transchelation step, enabling direct ^{99m}Tc transfer without separate reduction of MET. In vitro stability was demonstrated by fast protein liquid chromatography analysis of labeled MET-scFv, incubated with bovine serum albumin (BSA), transferrin and mouse serum. Last, in vivo pharmacokinetics, biodistribution and imaging were performed. **Results:** Yields of 6 mg/liter induced culture purified protein were achieved. Successful site-specific labeling was demonstrated using a Zn^{2+} transchelation modification of a pretinning method, which also enabled lower amounts of the reducing agent to be used. The specificity for CEA was retained after labeling. Despite a rapid serum clearance ($t_{1/2\alpha}$ = 2.8 min), adequate localization to tumor of 5.37% injected dose/g at 4 hr was demonstrated. Moreover, the short-lived $t_{1/2\alpha}$ of scFv, its early tumor targeting and rapid blood-pool clearance gave tumor-to-blood ratios of 2.07 by 4 hr, enabling early gamma camera imaging. Successful and specific imaging was achieved using LS-174T xenografts in nude mice by 3–6 hr. **Conclusion:** A recombinant MET containing scFv was successfully expressed, purified and labeled with ^{99m}Tc. The stable site-specific labeling of ^{99m}Tc, combined with the rapid plasma clearance of the scFv, led to successful early in vivo imaging of xenografted mice.

Key Words: immunoscintigraphy; single-chain antibody; imaging; CEA; recombinant antibody

J Nucl Med 1998; 39:47–56

The new imaging modalities of CT and MRI have, over the last 10 yr, made a significant impact on patient outcome, principally through better disease detection. Their influence, however, has not removed the clinical problem of inadequate treatment and treatment planning, which compromise patient outcome. Improper disease detection and understaging of disease extent remain important clinical problems that may contribute both directly and indirectly to patient outcome. Often, difficult and painful procedures, which are required to confirm or deny disease presence, would be unnecessary if a means for more sensitive and accurate detection were available. Examples are numerous. Insensitivity in detecting mediastinal nodal involvement in small-cell carcinoma of the lung often leads to thoracotomy for staging. The presence or absence of nodal involvement in breast carcinoma is so crucial to the overall treatment strategy and the detection of it in current conventional practice is so unreliable that axillary lymphadenectomy is commonly performed to properly stage the disease. Improved assessment of lymph nodes in early-stage prostatic cancer would lead to the more appropriate selection of patients for limited or more radical surgery. Each additional or more extensive initial surgery adds further to patient morbidity and mortality.

Radioimmunodetection (RAID) has emerged as a clinically useful field over the last 15 yr. Almost 200 clinical trials using RAID have been conducted during this time, with some clear and important findings (*1*). The greater facility of this technique to detect lesions deemed "occult" by conventional imaging was recognized even in early studies and has repeatedly been confirmed by studies, regardless of antibody, tumor or radionuclide type (*2*). Often, these tumors were found earlier than would be the case with other imaging techniques (*1,2*), with smaller lesions, often less than 2 cm, being more readily imaged. Although anatomical detail is excellent with conventional imaging, difficulties can be experienced in distinguishing normal contrasts within tissues and uninvolved nodal masses from malignancy. Radionuclides, because they are directed to tumor-associated antigens or to biologically distinct tumor targets, are more suited to making this distinction. Importantly, large studies have confirmed a 73% rate of true occult tumors, as opposed to a high false-positive detection rate (*1,3,4*).

Technetium-99m remains the imaging agent of choice. It has a gamma energy that is ideal for safe imaging (140 keV), is inexpensive and is readily available, being generator-produced and carrier-free. Its short half-life of 6 hr readily lends itself to coupling with antibody fragments for early imaging studies. Indium-111, with gamma emission energies of 173 keV and 247 keV, has qualities that also recommend it for imaging. Although it is also routinely available, difficulties remain with its coupling to antibody, which, in general, has been performed using a diethylenetriamine pentaacetic acid chelation method (*5*). Furthermore, it is expensive and has shown a tendency to accumulate in reticuloendothelial organs, liver and spleen (*1,5*). The iodine nuclides ^{131}I and ^{123}I may be both used for imaging and are readily conjugated to antibody, although, compared to ^{99m}Tc, both have problems. Iodine-131 has a high gamma energy emission (364 keV) and is long-lived, with a half-life of 8 days. Its component beta ray emission also complicates its

Received Nov. 4, 1996; revision accepted Apr. 7, 1997.

For correspondence or reprints contact: Geoffrey A. Pietersz, PhD, Austin Research Institute, Austin Hospital, Studley Road, Heidelberg, Victoria 3084, Australia.

toxicity. Iodine-123 (gamma emission, 159 keV) is expensive and is not readily available. Moreover, deiodination remains a problem with all direct oxidative methods of labeling using these nuclides, and although the rate and extent varies from method to method and between antibodies, deiodination remains the cause for uptake in thyroid, stomach and other normal organs (*6*). Indirect labeling using N-succinimidyl iodobenzoate (*7*) or an iodophenyl maleimide conjugate (*8*) result in better in vivo stability (*9*), although the synthesis of the precursor is laborious.

The use of smaller antibody fragments, $F(ab')_2$ and Fab', has led to the recognition of their capacity for early tumor targeting, with rapid clearance from blood and normal organs permitting the use of short-lived radionuclides and imaging within 6 hr (*10,11*). The sensitivity is also improved with fragments, as compared to intact IgG (*11,12*). In an intraindividual study comparing intact and fragmented anti-carcinoembryonic antigen (CEA) ^{99m}Tc-labeled antibody, the sensitivity of fragments, specifically a $F(ab')_2$/Fab' mix, was better at detecting primary tumors, local recurrences and metastases, including lymph node and liver metastases (*11*). The higher sensitivity of fragments in detecting early, smaller, better vascularized lesions is a result of the known ability of the fragments to diffuse and penetrate more easily in tissue and to be cleared faster from blood and nonspecific background to give better tumor-to-background ratios (*13–15*).

Single-chain antibody fragments (scFvs) have been shown to target tumors effectively, with a deeper penetration than other antibody forms, including fragments (*16*). The lack of Fc glycosylation permits bacterial expression of these molecules and enables novel fusion scFv proteins to be engineered by recombinant engineering techniques. Their small size and absence of constant region domains may contribute to lower immunogenicity, with theoretical advantages of less uptake by normal tissues through Fc receptors. Their rapid serum clearance permits a quick reduction in background counts with high tumor-to-blood ratios, enabling accurate imaging within 1–6 hr. A short-lived nuclide and a small antibody fragment with a half-life of minutes would make ideal partners, coupled as an imaging agent. Here, we describe the engineering of a metal-binding metallothionein (MET) peptide as part of a high-affinity, phage-selected anti-CEA scFv for use in the ^{99m}Tc RAID of experimental human colorectal xenografts. The C-terminal addition of a peptide for direct coordinate radiometal binding of ^{99m}Tc provides stable in vivo labeling without the technical inconveniences of chelate chemistry and is the basis for a novel diagnostic agent in this disease.

MATERIALS AND METHODS

Genetic Engineering

All kinase and ligase enzymes used were purchased from New England Biolabs, with digests performed in buffer solutions provided by the manufacturer. The MFE-23 plasmid is pUC19-based, with a *lacZ* promoter, an ampicillin resistance gene and a polycloning site (*17*). *Escherichia coli* TG1 (*supE hsd* Δ*5 thi* Δ (*lac-proAB*) F'[*tra* Δ 36 *proAB*$^+$ *lacI*^{q} *lacZ*Δ*M15*]) was used for plasmid propagation and expression of antibody fragments. Annealed oligonucleotides encoding for both MET (Lys-Cys-Cys-Thr-Cys-Ala) (*18*) and c-*myc* tag (Glu-Gln-Lys-Leu-Ile-Ser-Glu-Glu-Asp-Leu-Asn) were used to engineer these sequences into the C-terminal end of the light chain (V_L) of the phage-selected, anti-CEA, MFE-23 scFv (*17*). The c-*myc* sequence was used as a tag for purification of expressed protein using an anti-c-*myc* affinity column and it enabled protein analysis and detection in Western blots. Two complementary oligonucleotides were designed to have *Not*I and *Eco*RI overhangs at each end for directed cloning into the corresponding restriction sites within the vector. Sense (5'-G GCC GCA AAA TGT ACT TGT TGT GCT GAA CAA AAA CTC ATC TCA GAA GAG GAT CTG AAT TAA G-3') and antisense (5'-AA TTC TTA ATT CAG ATC CTC TTC TGA GAT GAG TTT TTG TTC AGC ACA ACA AGT ACA TTT TGC-3') oligonucleotides were synthesized by an Applied Biosystems 380A automated DNA synthesizer. This strategy required *Not*I and *Eco*RI digestion of the expression vector and phosphorylation of the oligonucleotides for annealing before ligation. The restriction digests of plasmid DNA were routinely performed in a 50- to 100-μl total volume containing 1–5 μg of DNA, using restriction buffers and under conditions as described by the manufacturer. The desired restriction enzyme was used in two- to threefold excess, and the reaction was incubated for 2–3 hr. Reactions were terminated by heat inactivation at 65°C for 15 min. DNA fragment purification was by low-melt agarose extraction. Phosphorylation of oligonucleotides for annealing by 10 units of T_4 polynucleotide kinase (10,000 units/ml) was performed in a 20-μl total reaction using 10× polynucleotide kinase (PNK) buffer (2 μl), 10m*M* ATP (2 μl) and 0.8 μg of each oligonucleotide. The reaction was left at 37°C for 30 min, both 5' sense and 3' antisense oligonucleotides were mixed and boiled for 5 min and the mixture was left to cool for annealing. Ligations were performed at room temperature for 4 hr in a 5-μl reaction using T_4 ligase. Transformed TG1 *E. coli* were screened and selected for by using an oligonucleotide (5'-ATG TAC TTG TTG TGC TGA AC-3') that was complementary to and spanned the MET and c-*myc* sequences. Confirmation of the nucleotide sequences was by dideoxy nucleotide sequencing over the *Not*I/*Eco*RI sites of successfully cloned TG1 *E. coli*.

Induction, Expression and Purification

Transformed *E. coli* were induced with 1 m*M* isopropyl-1-thio-β-D-galactopyranoside in an overnight induction at room temperature. The *E. coli* were grown at room temperature in 2× tryptone yeast (TY) medium containing 100 μg/ml ampicillin and 0.1 m*M* $ZnCl_2$, to an optical density, at 600 nm, of between 0.5 and 1.0 before induction. Cell fractions of the induced culture medium were then separated. The cell supernatant was first collected after an initial centifugation (12,500 rpm for 15 min). The outer membrane was subsequently permeabilized with 50 m*M* sodium phosphate, 100 m*M* NaCl, 1 m*M* EDTA and the periplasmic fraction collected as the supernatant of a further centrifugation (12,500 rpm for 15 min). Finally, the remaining pellet was sonicated after resuspension in phosphate-buffered saline (PBS) and spun as above, and the cytoplasmic component collected as the supernatant of a final centrifugation (12,500 rpm for 15 min).

The expressed proteins were visualized after purification using sodium dodecyl sulfate (SDS)-15% polyacrylamide gel electrophoresis; the gel was stained with Coomassie blue and analyzed by Western blot with an anti-tag mouse monoclonal antibody. Purification of the recombinant protein was by affinity chromatography, using a mouse monoclonal anti-tag antibody linked to tosyl-activated agarose (Pierce, Rockford, IL). Diethylamine (50 m*M*) and 0.5 *M* NaCl were used for the elution of bound protein. The positive fractions, detected by anti-tag antibody in a dot-blot horseradish peroxidase (HRP)-enhanced chemiluminescence, were combined. These pooled samples were concentrated by an Amicon (Beverly, MA) concentrator to a final volume of 2–5 ml. Purified scFv was transferred from SDS-15% polyacrylamide gels to Immobilon-P (Millipore, Bedford, MA), using a mini-transblot apparatus (Bio-Rad, Hercules, CA). Membranes were blocked in 5% casein, either overnight at 4°C or at room temperature for 1 hr.

Monoclonal murine anti-tag primary antibody was added to the membrane and bound murine antibody was detected with HRP-labeled sheep anti-mouse secondary antibody (Amersham, Buckinghamshire, England). Blots were developed using the Amersham enhanced chemiluminescence reagent. Estimation of purified scFv was by absorbance at 280 nm, using an extinction coefficient of 0.71, calculated from the sum of the extinction coefficients of tryptophan, tyrosine and cysteine residues within the protein (*19*).

Antigen-Binding Studies

The antigen specificity of MET-scFv was tested by fluorescence-activated cell sorting (FACS), using a CEA-expressing cell line, LS-174T (*20*), and by both enzyme-linked immunosorbent assay (ELISA) and radioimmunoassay (RIA), using a solid-phase antigen. Fluorescence-activated cell sorting analysis was performed as follows. LS-174T cells (1×10^6) were incubated with an appropriate amount and volume of scFv, serially diluted and left at 4°C for 60 min. Cells were washed three times with 1× PBS, containing 0.025% NaN_3 and 2% BSA, and incubated with the mouse anti-tag monoclonal antibody for a further 60 min at 4°C. Analysis using a Becton Dickinson FACScan (Becton Dickenson Immunocytometry Systems, Mountain View, CA) was done after further washing and a 60-min incubation at 4°C with a sheep anti-mouse fluorescein isothiocyanate-conjugated $F(ab')_2$ (Silenius Laboratories, Hawthorn, Victoria, Australia).

Enzyme-linked immunosorbent assays and RIAs were performed in the following manner. Flat-bottomed, 96-well plates (Costar, Cambridge, MA) were coated overnight at 4°C with 50 μl/well purified CEA (10 μg/ml) in carbonate/bicarbonate buffer (pH 9.6). After washing in PBS containing 0.05% Tween 20 (PBS/T20), all wells were blocked by incubation with 200 μl/well 1% BSA (PBS/BSA). The scFv at 50 μl/well then was added and serially diluted twofold across the wells. Wells were incubated for 1 hr at 25°C and then washed with PBS/T20, secondary anti-tag antibody was added (1 hr at 25°C) and, after a further wash, sheep anti-mouse HRP-labeled immunoglobulin (Amersham, Buckinghamshire, England), diluted 1:500, was added (1 hr at 25°C). All washes with PBS/T20 were performed 5–10 times. Bound enzymatic activity was determined photometrically at 405 nm using the peroxidase dependent reaction of H_2O_2 and 2′,2-azino-di-(3-ethylbenzthiazoline sulfonate). This was prepared as a 25× stock (15 mg/ml in water), stored at 20°C and diluted to 1× with 0.1 *M* citric acid (pH 4.0), to which 0.005% H_2O_2 was added immediately before use. A similar protocol was followed for evaluation of ^{99m}Tc-labeled scFv binding, except that, after incubation (1 hr at 4°C) and washing with PBS/T20, individual wells were excised and bound radioactivity was counted using a gamma counter (1260 Multigamma Counter; Wallac, Oy, Finland).

The kinetics of binding for the construct were measured on a BIAcore 2000 machine (Pharmacia, Uppsala, Sweden). Association and dissociation rates were measured using an aldehyde-coupled CEA chip, as outlined in the manufacturer's protocols (BIApplications Handbook, Biosensor, Pharmacia) and previously by other investigators (*21*). An antigen density of 2000 resonance units (RU) was used with serial dilutions of scFv and IgG-JGT (an intact IgG anti-CEA used as the positive control for the FACS analysis) (*22*), from 100 to 1000 n*M*, in binding buffer Hepes buffered saline (HBS) /p20 at a flow rate of 5 μl/min. Kinetic evaluation was performed using the BIAevaluation software, version 2 (Biosensor, Pharmacia).

Labeling

Technetium. A modification of a pretinning method was used (*23,24*). For in vitro characterization experiments, TcO_4^-, eluted from the generator, was diluted to 100 μCi/100 μl with normal saline. TcO_4^- was reduced to ^{99m}Tc by the addition of 20 μl of 5 × 10^{-4} *M* $SnCl_2$/0.1 *M* HCl (for non-Zn^{2+}-chelated MET-scFv) or 6.25×10^{-5} *M* $SnCl_2$/0.1 *M* HCl (for Zn^{2+}-chelated MET-scFv) and left to incubate at room temperature for 15 min. To this mix was added 100 μl of MET-scFv (1 mg/ml), and after 60 min, the solution was filtered through a 0.22-μm filter (Millipore). Purification of free ^{99m}Tc from labeled protein was performed by gel filtration. Excess ^{99m}Tc was removed, for RIA studies, by passage through a PD10 Sephadex G25 column or, for imaging by fast protein liquid chromatograhy (FPLC), using a TSK 2000 column (7.8 mm × 30 cm; Bio-Rad). Fractions in each case with the highest activity were pooled and used for further studies. Depending on generator availability, eluted TcO_4^-, in the same quantities and reactions as documented above, was used neat at between 25 and 30 mCi for in vivo imaging experiments.

Iodination. Iodination of MET-scFv was by Iodobeads (Pierce). MET-scFv (100 μl) was added to 3 μl of $Na^{125}I$ (100 mCi/ml; Amersham) in the presence of a single Iodobead. After 10 min, free ^{125}I was removed by size-exclusion chromatography through a PD10 column (Pharmacia, Sweden).

Immunoreactivity. The immunoreactive fraction of labeled antibody was determined on a CEA-Sepharose beads after labeling. Briefly, the labeled scFv (100 μl) was applied onto CEA-Sepharose and counted in a gamma scintillation counter (1260 Multigamma Counter) after a 2-hr incubation at 4°C. The beads were then washed with 1% BSA, until counts were negligible in the supernatant. The radioactivity remaining in the beads was measured, and the percentage bound was calculated.

Stability

The integrity of the labeled protein after incubation in 80% mouse serum was studied by trichloroacetic acid (TCA) precipitation over time. Serum (100 μl) and labeled ^{99m}Tc-MET-scFv were added to an equivalent amount of 40% TCA. The mix was left on ice for 10 min and spun for 3 min at 15,000 rpm, and the pellet was subsequently washed twice with 20% TCA and acetone (1 ml) and counted directly on a gamma counter (1260 Multigamma Counter). Transchelation experiments were conducted by FPLC analysis (TSK 2000 column) of labeled MET-scFv, postincubated with BSA, transferrin or normal mouse serum for 4 hr. Protein (spectrophometry reading at 280 nm) and radioactive counts of the collected fractions were measured and plotted.

Animal Studies

Mice and Tumors. Female severe combined immunodeficiency (SCID) mice (Animal Resources Center, Perth, Western Australia, Australia) were used for the pharmacokinetic and biodistribution studies. Female BALB/c nude mice (Biological Research Laboratories, Austin Hospital, Heidelberg, Victoria, Australia) were used in the imaging work. Tumor cells used in the following studies were from the CEA-expressing human colorectal tumor line LS-174T (*25*) and the non-CEA-expressing murine thymoma line E3 (*26*). All cell cultures were maintained in Dulbecco's modified Eagle's medium or RPMI medium (Commonwealth Serum Laboratories, Sydney, New South Wales, Australia), supplemented with 10% heat-inactivated fetal calf serum, 2 m*M* glutamine (Commonwealth Serum Laboratories), 100 μg/ml streptomycin (Glaxo, Melbourne, Victoria, Australia) and 100 units/ml penicillin (Commonwealth Serum Laboratories).

Pharmacokinetics. Mice were injected intravenously with 0.7 μCi of ^{125}I-labeled MET-scFv and bled by eye bleeds at various times for all blood clearance studies. Three mice were used per time point. The data were analyzed using GraphPad software and a nonlinear regression analysis.

Biodistribution Studies. The biodistribution of labeled MET-scFv (0.70 μCi of ^{125}I) and (0.6 μCi of ^{99m}Tc) were conducted on LS-174T tumor-bearing mice when tumors were 0.4–0.5 cm in

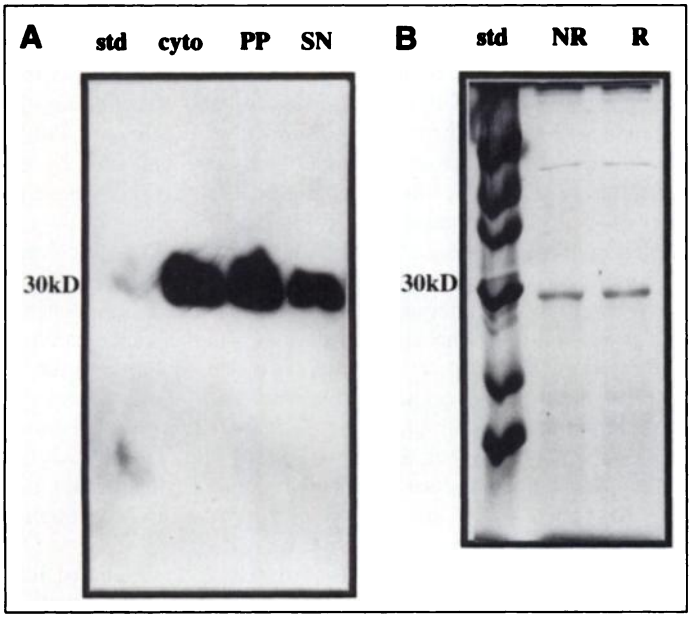

FIGURE 1. (A) Western blot of cellular fractions from induced *E. coli.* (B) Coomassie blue-stained SDS-15% polyacrylamide gel of purified MET-scFv under reduced (Lane R) and nonreducing (Lane NR) conditions.

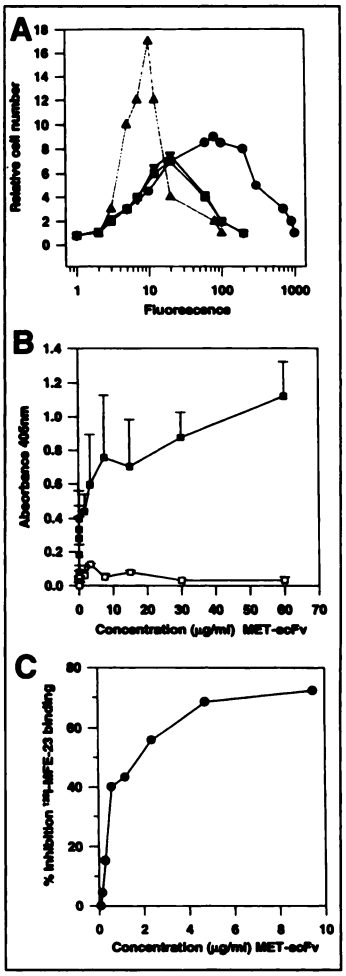

FIGURE 2. (A) FACS, comparing binding of intact anti-CEA IgG-JGT (●), MET-scFv (▼), MFE-23 scFv (■) and LS-174T cells alone (▲) to LS-174T cells. (B) Binding of unlabeled MET-scFv on plates coated with CEA (■) and BSA (□). Bars represent the s.d. of results. (C) Competitive ELISA using unlabeled MET-scFv to inhibit the binding of iodinated (^{125}I) MFE-23 to CEA-coated plates.

diameter. All mice were injected intravenously through the tail vein. Mice (three or four per data point) were killed at 24 and 48 hr (^{125}I) and 4 and 24 hr (^{99m}Tc). After death by cervical dislocation, blood, all major organs and tumors were weighed using an analytical balance and counted in a gamma scintillation counter (1260 Multigamma Counter).

Imaging. In general, tumors of 1 cm^2 were imaged unless otherwise stated. Intraperitoneal injection of 0.5 ml of FPLC-purified, ^{99m}Tc-labeled MET-scFv (4.5–5 μCi) was used to obtain images at the times outlined in the text. Mice were anesthetized using intraperitoneally-injected Rompun (20 mg/ml xylazine)/ Ketavet 100 (100 mg/ml ketamine) mix (0.5 ml of each). The mixture was added to 10 ml of PBS, and 0.4 ml of mixture was added per 20 g of mouse body weight. Imaging was by a Siemans ZLC 7500 gamma camera using a low-energy, all-purpose collimator. Each mouse was imaged for 10 min.

RESULTS

Engineering of MET-scFv

The MFE-23 pUC19-based vector (*17*) was modified to include the MET (Lys-Cys-Cys-Thr-Cys-Ala) and c-*myc* tag sequences (Glu-Gln-Lys-Leu-Ile-Ser-Glu-Glu-Asp-Leu-Asn) at the C-terminal end of the V_L chain. This was done by directed ligation of an oligonucleotide duplex with matching 5′ *Not*I and 3′ *Eco*RI restriction sites into similar sites in the polycloning region of the original vector.

Expression and Purification

Soluble MET-scFv expression, as demonstrated by Western blot analysis, was evident in all subcellular fractions (Fig. 1A). Expressed protein from all cellular compartments was combined and purified on an anti-tag affinity column. Samples, after dialysis into PBS postelution, were concentrated in an Amicon concentrator. A yield of approximately 6 mg/liter induced culture of the purified MET-scFv was obtained. Analysis of the purified protein on SDS-15% polyacrylamide gels under reducing and nonreduced conditions (Fig. 1B) demonstrated an absence of larger molecular weight forms, consistent with the lack of disulfide-linked polymers.

Binding

Cellular and solid-phase assays were used to demonstrate specificity of the MET-scFv recombinant protein for CEA. Binding of MET-scFv to CEA expressing LS-174T cells was evident on FACS analysis, with a clear difference in fluorescence between CEA-expressing cells with surface-bound MET-scFv and those without the addition of the scFv antibody (Fig. 2A). No binding to non-CEA-expressing E3 cells was shown (data not shown). The greater fluorescence with intact murine anti-CEA control immunoglobulin, IgG-JGT, compared to the engineered monovalent fragment, was not a surprise and was in keeping with published data indicating a loss of four- to tenfold in affinity between parent immunoglobulin and its monovalent forms (*27,28*). Enzyme-linked immunosorbent assay readings also maintained specificity of the construct for CEA, with no detectable binding to BSA (Fig. 2B) and up to 75% inhibition of binding to CEA of the unaltered MFE-23 scFv by the recombinantly engineered MET-scFv (Fig. 2C).

BIAcore Analysis and Affinity Constants

The binding characteristics of MET-scFv were measured by surface plasmon resonance using a BIAcore 2000 machine (Biosensor, Pharmacia). Binding of MFE-23-scFv, MET-scFv and an intact murine anti-CEA immunoglobulin, IgG-JGT, were compared. Notably, there was little difference in the affinity constant (K_D) between MFE-23-scFv and the engineered MET-scFv: $2.43 \times 10^7\ M^{-1}$ and $2.34 \times 10^7\ M^{-1}$, respectively (Table 1). The slightly lower association rate for MET-scFv $2.20 \times 10^3\ M^{-1}\cdot sec^{-1}$, was compensated for by a slower rate of dissociation, $0.94 \times 10^{-4}\ M^{-1}$, compared to MFE-23-scFv, with rates of $3.96 \times 10^3\ M^{-1}\cdot sec^{-1}$ and $1.63 \times$

TABLE 1
Analysis of Binding Kinetics

Antibody	$k_{(on)}$ $M^{-1}s^{-1}\times10^{-3}$	$k_{(off)}$ $M^{-1}\times10^{4}$	K_D $M^{-1}\times10^{-7}$	K_D $M^{-1}\times10^{-7}$ (Scatchard)
MFE-23-scFv	3.96 ± 0.79	1.63 ± 0.28	2.43 ± 0.90	5.1 ± 0.74
MET-scFv	2.20 ± 0.36	0.94 ± 0.15	2.34 ± 0.75	3.0 ± 0.48
IgG JGT	30.9 ± 12.8	0.68 ± 0.15	45.7 ± 28.8	ND

10^{-4} M^{-1}, respectively. The lack of difference in affinity constants was confirmed on measurement of the K_D by Scatchard analysis (*29*) (Table 1). A likely cause for the lower K_D of scFvs, in general, compared to intact IgG, was the lower rate of association and faster dissociation rate of the scFv constructs compared to IgG-JGT (Table 1).

Labeling

The specific activity of ^{99m}Tc labeling was between 0.5 and 0.75 μCi/μg, depending on the concentration of the generator eluate. Immunoreactivity measured on CEA-Sepharose beads was 82% of the labeled product. The optimum pH for labeling was 3 (results not shown). $SnCl_2$ was used in a standard pretinning method (*24*) for reduction of TcO_4^- and the metal-chelating MET site. Of initial interest was the observation that scFv with the engineered MET site did not confer a higher degree of ^{99m}Tc binding, when compared to the unaltered MFE-23-scFv from which it was derived (Fig. 3A). This was explicable through the exposure of —SH groups and other groups, discussed later, throughout the molecule, by $SnCl_2$ reduction with a non-site-specific binding of ^{99m}Tc. Such labeling is less secure than the coordinate binding of ^{99m}Tc to MET (*30,31*) and is, thus, more susceptible to transchelation, both in vitro and in vivo, and may, indeed, interfere with site-specific labeling to the MET site.

This presumed nonspecificity of ^{99m}Tc binding was confirmed by in vitro transchelation experiments using 25 m*M* cysteine. After $SnCl_2$ labeling, both MFE-23-scFv and MET-scFv were exposed to 25 m*M* cysteine for 1 hr, and binding was reassayed by RIA. A significant transfer of weakly bound ^{99m}Tc from both constructs to cysteine was demonstrated, with a significant lowering of counts (Fig. 3A). A slight advantage of ^{99m}Tc binding is, however, seen for the MET (MET-scFv) antibody (Fig. 3A).

To enable a more specific labeling of the MET site and to limit the exposure of general ^{99m}Tc-binding groups, a method was sought to protect this site from oxidation during bacterial soluble expression. The use of Zn^{2+} (0.1 m*M*) during the induction phase of the recombinant scFv growth served as a means of protecting the metal-binding site in a reduced state through the binding of Zn^{2+}. The greater natural affinity of MET for ^{99m}Tc (*32*) then enabled a direct transchelation of ^{99m}Tc for Zn^{2+}, without the need for a reduction of the entire MET-scFv and the attendant nonspecific binding of ^{99m}Tc. This enabled the use of a $SnCl_2$ solution of weaker concentration for labeling. Notably, the amount of $SnCl_2$ was reduced from 5.0×10^{-4} *M* to 6.25×10^{-5} *M* for subsequent experiments, essentially to reduce TcO_4^- to ^{99m}Tc for labeling.

The effect of this Zn^{2+} protection of the MET site on the stability of the labeled MET-scFv was clearly evident (Fig. 3B). Labeled MET-scFv (Zn^{2+}-chelated), was minimally affected by coincubation with 25 m*M* cysteine. In direct contrast was the poor labeling of the MET-scFv without Zn^{2+}, with an almost complete transfer of label to cysteine (Fig. 3B). The lack of a protected site specific metal-binding site did not permit reduction of other nonspecific sites using the lower $SnCl_2$ concentration with a correspondingly poor labeling. Analysis of the labeled MET-scFv (Zn^{2+}-chelated) by FPLC analysis (Fig. 3C) demonstrated a single predominant peak at M_r 30,000. Notably, there was no evidence of multimer formation (confirmed by nonreducing SDS-polyacrylamide gel electrophoresis; results not shown) or substantial colloid. In total, 95.4% of the nonfree counts were associated with the MET-scFv peak. The late peak represented unlabeled free ^{99m}Tc. Specificity of the ^{99m}Tc-labeled MET-scFv (Zn^{2+} chelated) was retained for CEA, as seen on direct binding to CEA-coated RIA plates (Fig. 4A) and confirmed by inhibition of binding of labeled MET-scFv by "cold" MFE23-scFv to CEA plates, by up to 70% (Fig. 4B).

In Vitro Stability

Before in vivo imaging experiments, the in vitro stability of labeled MET-scFv (Zn^{2+}-chelated) was tested. In TCA precipitation experiments, after co-incubation with 80% normal mouse serum at 37°C, 80% remained protein bound 3 hr postincubation (data not shown). To test that there was no transfer of ^{99m}Tc to other proteins, FPLC analyses of labeled MET-scFv (Zn^{2+}-chelated), after incubation with BSA, transferrin or normal mouse serum, were performed separately (Fig. 5, A, B and C, respectively). After a 4-hr incubation, the radioactive peak remained unchanged from the expected protein

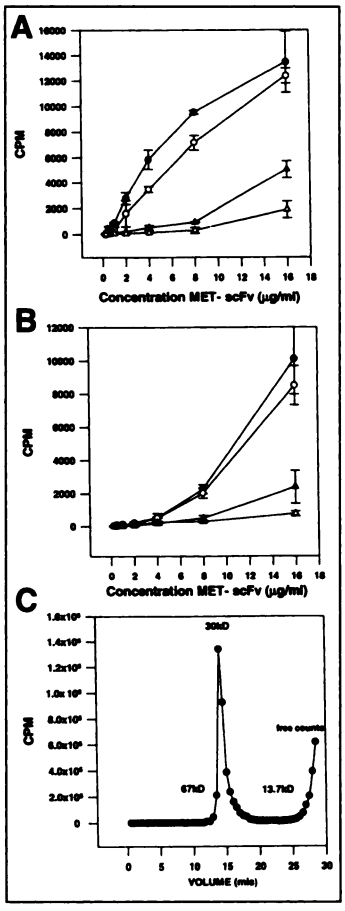

FIGURE 3. (A) Comparison of binding to CEA of directly labeled ^{99m}Tc-labeled MET-scFv, both before (●) and after (▲) the addition of 25 m*M* cysteine with non-MET-containing anti-CEA scFv MFE-23 before (○) and after (△) the addition of 25 m*M* cysteine. Bars represent the s.d. of the mean. (B) Comparison of binding to CEA of ^{99m}Tc-labeled MET-scFv using Zn^{2+} transchelation before (●) and after (○) the addition of 25 m*M* cysteine with a ^{99m}Tc-labeled MET-scFv without Zn^{2+} transchelation before (▲) and after (△) the addition of 25 m*M* cysteine. Bars represent the s.d. of the mean. (C) FPLC (TSK 2000 column) profile of ^{99m}Tc-labeled, Zn^{2+} transchelated MET-scFv.

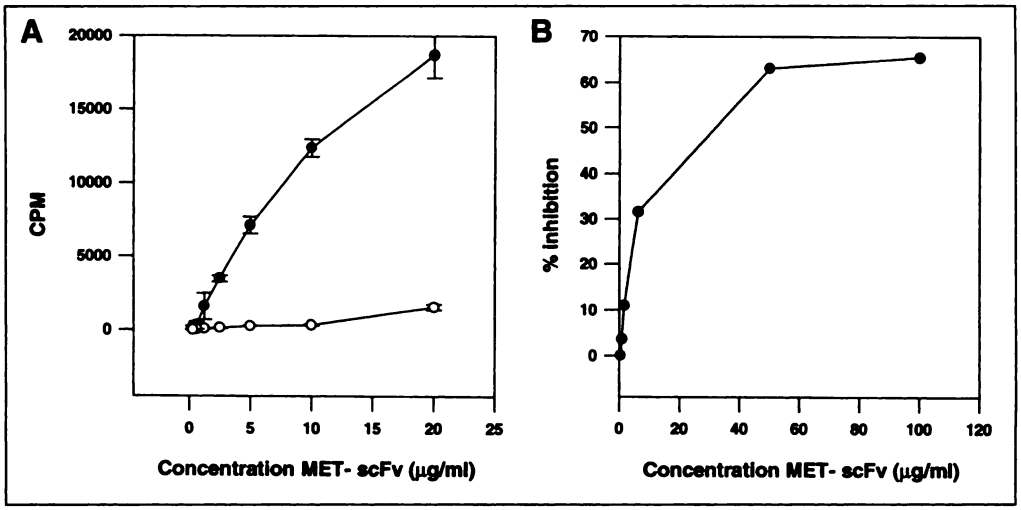

FIGURE 4. (A) Binding of ^{99m}Tc-labeled MET-scFv on plates coated with CEA (●) and BSA (○). Bars represent the s.d. of the results. (B) Competition binding of ^{99m}Tc-labeled MET-scFv on CEA using unlabeled MFE-23 scFv.

peak for MET-scFv of 30 kDa in each instance. No transfer of counts to the expected protein peak for BSA, transferrin or mouse serum was seen (Fig. 5, A, B and C, respectively).

Serum Clearance and Biodistribution

For rapid and distinct images, high tumor-to-blood ratios with a rapid serum clearance are desired properties, for which scFvs, in general, are suited (*10,11*). The MET-scFv antibody demonstrated a rapid serum clearance with a biphasic elimination ($t_{1/2\alpha}$ = 2.8 min). The biodistribution data (Fig. 6A) also were favorable, with regard to imaging prospects for this construct. By 4 hr, a high tumor localization was seen at 5.37% injected dose/g (%ID/g), which rapidly fell to 1.69%ID/g by 24 hr. The early targeting to tumor, combined with the very short plasma $t_{1/2}$ and the short-lived radiation characteristics of ^{99m}Tc, led to tumor-to-blood ratios of 2.07, even by 4 hr, permitting rapid gamma camera imaging (Fig. 6, B and C). Although renal, splenic, hepatic and, to a lesser extent, gastric uptake was high at 4 hr (9.96%, 5.11%, 4.09% and 3.61% ID/g, respectively) over time, these absolute levels fell to low levels by 24 hr (0.3%, 0.41%, 0.12%, and 0.08% ID/g) (Fig. 6A). This also was evident in the tumor-to-tissue levels measured at 4 and 24 hr postadministration (Fig. 6C), which showed significant increases, except in spleen, liver and bone. Notably, a marked loss of activity was noted in the kidney, with a 32-fold increase in the tumor-to-tissue ratio for this organ by 24 hr.

The suitability of a ^{99m}Tc-labeled construct, compared to a ^{125}I label, was evaluated by a comparative biodistribution evaluation (Fig. 7A). All organs demonstrated a higher level of ^{125}I-labeled MET-scFv than did ^{99m}Tc-labeled scFv (Zn^{2+}-chelated), which would presumably relate to both the slower blood clearance of iodinated species and the more rapid decay of ^{99m}Tc (*33*). The rapid serum clearance of ^{99m}Tc-labeled scFv, however, led to a 2.7 times higher tumor-to-blood ratio at 24 hr than that for ^{125}I-scFv ($p < 0.001$) (Fig. 7B). Of note was the high splenic uptake using both radiolabels. This has been noted in previous work by this laboratory, using different antibodies in SCID mice (*34,35*), and has been attributed to the SCID phenotype, independent of antibody denaturation. The accumulation of scFv would indicate that this characteristic is independent of an Fc receptor-mediated process, and this observation led to the use of nude mice in subsequent imaging experiments.

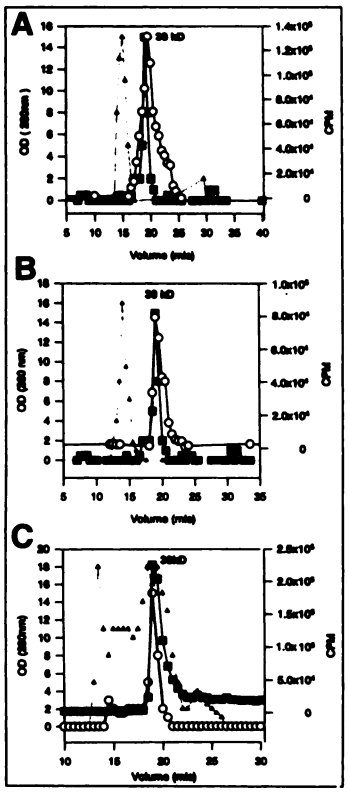

FIGURE 5. Stability of ^{99m}Tc-labeled MET-scFv. The optical density FPLC profiles of co-incubated proteins read at 280 nm (△) are shown with the corresponding radioactivity profiles of ^{99m}Tc-labeled, Zn-chelated MET-scFv both before (■) and after (○) a 4-hr co-incubation period. (A) BSA; (B) transferrin; and (C) mouse serum.

Imaging

Imaging studies were conducted on nude mice xenografted with a human CEA-expressing colon cancer line, LS-174T (Fig. 8). A 0.5 × 0.5-cm tumor, grown subcutaneously on the dorsum of the neck, was clearly imaged at 2 and 6 hr after intraperitoneal injection (Fig. 8A). Uptake in heart (blood pool), spleen and peritoneum at 2 hr was significantly decreased by 6 hr, with a relative retention of the isotope in the tumor. Specificity of targeting was demonstrated by imaging a nude mouse with both a CEA-expressing tumor (head, 0.2 × 0.2 cm) and an irrelevant E3 tumor (grown in the lower left abdomen, 0.3 × 0.3 cm, but seen on the right, as indicated, because of image inversion) grown concurrently (Fig. 8B). Imaging was performed at 1 and 6 hr after intraperitoneal injection. Localization to the CEA-expressing tumor on the head without specific abdominal localization to the E3 tumor was notable. Again, increased relative tumor retention was seen with the time indicative of the increasing tumor-to-blood ratio from 1 to 6 hr. The decreased intensity of the tumor image compared to that observed in Figure 8A was explicable in terms of the relative sizes of the tumors imaged. The tumor in Figure 8B was 1/6 the size of that imaged in Figure 8A and was noteworthy in the successful

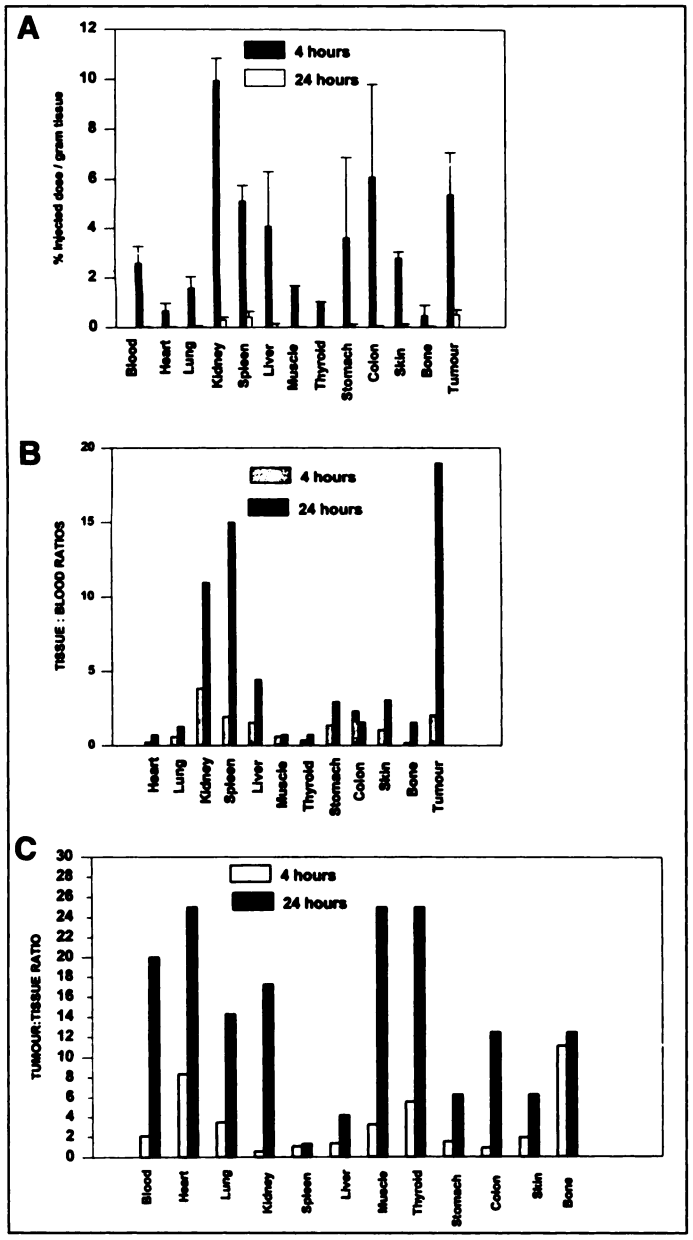

FIGURE 6. (A) Biodistribution of ^{99m}Tc-labeled MET-scFv in SCID mice bearing xenografted LS-174T tumor cells. Bars represent the s.d. of the results. (B) Tissue-to-blood ratios of ^{99m}Tc-labeled MET-scFv from A at 4 and 24 hr. (C) Tumor-to-tissue ratios of ^{99m}Tc-labeled MET-scFv from A at 4 and 24 hr.

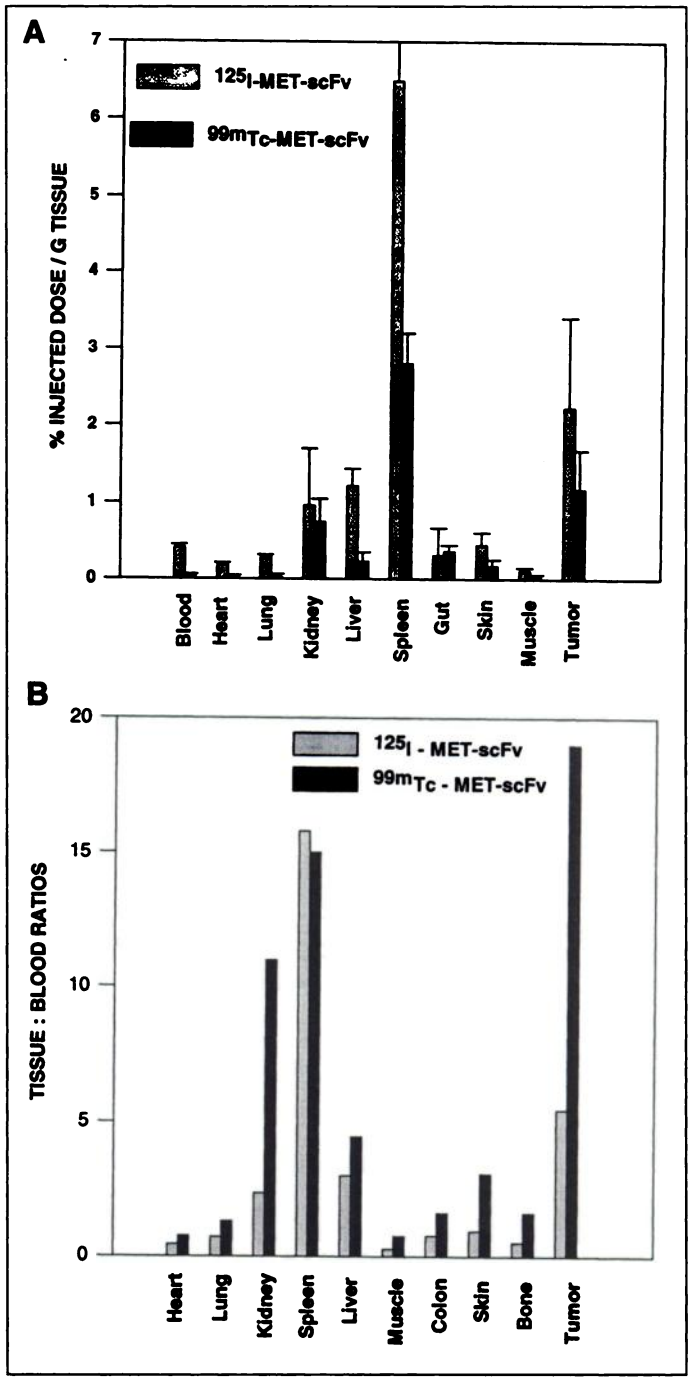

FIGURE 7. (A) Comparison of the biodistribution between ^{99m}Tc-labeled and ^{125}I-labeled MET-scFv forms in LS-174T xenografted SCID mice. Bars represent the s.d. of the results. (B) Comparison of tissue-to-blood ratios of ^{99m}Tc-labeled and ^{125}I-labeled MET-scFv from A.

localization and visualization with a lower tumor burden. Noteworthy also was the lower splenic uptake in nude mice than would be indicated by the biodistribution data performed in SCID mice.

DISCUSSION

Here, we discuss the production of an anti-CEA single-chain antibody that is capable of direct labeling with ^{99m}Tc using an affinity-purified, phage-expressed scFv, MFE-23 (*17*). The MET peptide sequence was cloned into the C-terminal end of the variable region of the light chain (V_L) using standard recombinant technology and successfully expressed in soluble secreted form in *E. coli.* A one-step purification by affinity chromatography was achieved to give yields of 6 mg/liter induced culture. Labeling of the MET-scFv construct, using an intermediate Zn^{2+} chelation step, followed by transchelation with ^{99m}Tc using a pretinning method, was used (*24*). Site-specific, stable binding of ^{99m}Tc was demonstrated in vitro with a high immunoreactivity of 82%. Size-exclusion FPLC after incubation of the labeled fragment in serum did not indicate transchelation to other serum proteins.

Successful tumor localization using human colon tumor–nude mouse xenograft models was demonstrated in preclinical in vivo experiments. Early targeting to tumor combined with a very short serum half-life of 2.8 min ($t_{1/2\alpha}$), resulted in tumor-to-blood ratios of over 2.0 by 4 hr. The slower clearance of antigen-bound label compared to unbound ^{99m}Tc led to improved images at 6 hr because of a more rapid clearance from the blood pool and a rapid reduction in %ID/g values for normal tissues by 24 hr. In vivo specificity of tumor targeting to CEA-expressing tumor also was shown.

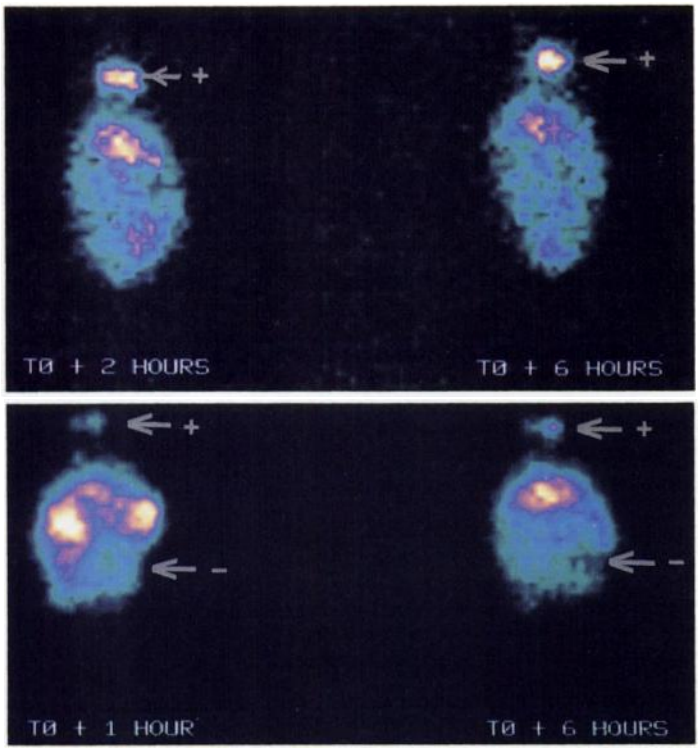

FIGURE 8. (A) In vivo imaging studies of xenografted LS-174T cells in nude mice (subcutaneously on the head) using ^{99m}Tc-labeled MET-scFv at 2 and 5 hr. (B) In vivo imaging, again in nude mice, with dual-xenografted subcutaneous tumors. CEA-expressing (+) LS-174T cells (head) and E3, non-CEA-expressing cells (−) (seen on the right flank in the image).

Our yield of purified protein, 6 mg/liter, is in accord with other studies of secreted recombinant proteins (*36–38*). The specificity of the MET-scFv fusion protein for CEA is retained without significant change in the binding kinetics from the parent MFE-23 scFv (Table 1). This is indicative of the lack of disruption to the antigen-binding site of the scFv component of the hybrid protein after the addition of MET peptide, as has been noted previously (*33,39,40*)

Several advantages are associated with the labeling of this MET-scFv antibody fragment. First, the use of Zn^{2+} to prebind, during the induction phase, the sulfhydryl groups of the cysteine residues in the MET peptide enables them to be maintained in a reduced form before the transchelation with ^{99m}Tc. This permits the use of milder reducing conditions for labeling, in essence, only to generate ^{99m}Tc from TcO_4^-. The requirement for exposed disulfide bonds for direct labeling may lead to harsh reducing conditions, often with the disruption of intrachain disulfide bridges, which can affect the immunoreactivity of the labeled product (*41*). Milder reduction conditions are more likely to preserve antibody function. The high immunoreactivity of 82% was in keeping with this assumption and is at the high end of other recorded results which vary from 70% to 85% for ^{99m}Tc-labeled fragments (*10,42*).

Second, this method permits site-specific ^{99m}Tc binding without a need for indirect bifunctional chelating agents. This avoids the chemical problems of using such agents (diethylenetriamine pentaacetic acid, bisthiosemicarbazones and diamide dimercaptide N_2S_2 ligands), which include expense, difficulties of purification and immunogenicity when bound to antibody (*9,43,44*). The chelate, when chemically bound to antibody, also may react randomly with several groups on the molecule, including within the hypervariable region and the antigen-binding site, inactivating antibody affinity or specificity (*45*).

Last, the site-specific ^{99m}Tc coordination to the MET site, using the Zn^{2+} transchelation methodology, reduces the nonspecific nature of ^{99m}Tc binding when pretinning radiolabeling methods are used. Apart from the native sulfhydryl groups, other endogenous donor groups on the antibody molecule, to which reduced ^{99m}Tc ions may bind, include terminal amino groups of N-terminal amino acids and ϵ-amino groups of lysine residues (*46–48*). Although direct methods offer advantages of simplicity, the nonuniform binding of ^{99m}Tc to sites of different affinities can lead to labile metal–antibody linkages, subject to in vivo breakdown and transchelation to serum proteins. This can have significant effects on biodistribution, with increased background levels of radioactivity and lower target uptake, leading to poor imaging (*31,49*). Stability of our labeled MET-scFv was demonstrated initially to sulfhydryl-containing molecules, such as cysteine (Fig. 3B). Plasma levels of free cysteine have been reported as 10 μM (*50*) with tissue concentrations in the range of 10–100 μM (*51*). These levels may affect in vivo clearance and tissue localization (*41*) of weakly bound ^{99m}Tc.

The relative stability of Zn^{2+}-protected MET-scFv, labeled by ^{99m}Tc transchelation, compared to directly reduced MET-scFv (Fig. 3B) suggests that our fragment would be less influenced by other sulfur-containing molecules in vivo. Others also have shown the greater fragility of directly ^{99m}Tc-labeled antibody compared to indirect methods (*41*). Evidence for the greater stability of our site-specific, Zn^{2+}-transchelated, ^{99m}Tc-labeled scFv was further strengthened by the FPLC analysis after incubation with normal mouse serum and transferrin (Fig. 5). No change in the radioactive peak was observed after 4 hr incubation. Uptake in liver, spleen and urine was, however, noted in the biodistribution studies (Fig. 7) and in the in vivo imaging experiments (Fig. 8). Given that bile and urine are a major excretion pathway for sulfur-containing compounds (*52,53*), transchelation to plasma cysteine or glutathione would account for some of this uptake and would indicate that optimization of labeling needs still further refinement. The incorporation of multiple MET sites would also be of interest in assessing labeling stability. The large fall in renal activity from 4 to 24 hr would be in keeping with the initial rapid excretion of scFvs in general by the kidneys noted by others (*16,28,54*)

A comparison of our MET-scFv with another scFv-fusion protein capable of binding ^{99m}Tc through a C-terminal cysteinyl peptide (Gly_4Cys) revealed similar in vitro properties (*33*). Metallothionein peptide has three cysteine residues in close proximity and could, theoretically, have a stronger affinity for ^{99m}Tc (*55*). Stability studies, using FPLC analysis, after protein or serum incubation, would be of interest with the Gly_4Cys 26-10-1 sFv′ fusion protein because this was not described, especially because the use of a $SnCl_2$ pretinning direct labeling procedure could lead to binding to low-affinity sites in the construct away from the engineered site.

CONCLUSION

The benefits of ^{99m}Tc as a nuclide for imaging have already been espoused. Comparing ^{125}I-labeled to ^{99m}Tc-labeled MET-scFv in biodistribution studies highlighted these advantages. Normal tissue and tumors showed higher %ID/g values with ^{125}I-Met-scFv, but the more rapid serum clearance of ^{99m}Tc-MET-scFv led to better tumor-to-blood ratios at the time points measured (Fig. 7). This difference, with respect to antigen targeting and normal tissue uptake, is even more striking on comparing complete and fragmented monoclonal antibodies, all labeled with ^{99m}Tc (*56*). Intact ^{99m}Tc-labeled immunoglobulin showed a slow continuous uptake throughout a 24-hr period with, in contrast, only a short uptake during the first 4 hr with

similarly labeled fragments. Normal tissues also demonstrated a continuous uptake over time, whereas, after the first hour postinjection, a washout of nonspecific binding predominated with the fragments. The low absolute amount of antibody uptake with fragments resulted in a lower percentage of lesions being visible with planar scans, although the higher tumor-to-background readings led to greater overall sensitivities. The refinement of image registration techniques using combination images from CT/MRI and SPECT will only enhance the use of fragments in imaging studies.

Metallothioneins are a series of single-chain proteins of about 6–7 kDa, conserved, to a great extent, throughout many species. It is thought they function as metal-detoxifying agents (*18*). It has been found that they have a low immunogenicity using cross-linked antibody conjugates in monkeys (*57*). The number and proximity of cysteine residues permit a strong metal coordination. The possibilities of metal binding extend beyond just the use of ^{99m}Tc. Rhenium, the element below technetium in the periodic table, shows a similar chemistry and allows an extension of the methodology used here to labeling scFv with the two rhenium isotopes, ^{186}Re and ^{188}Re. Rhenium-186 has a half-life of 90 hr, with both 1074-keV beta-emission and a 137-keV gamma-emission characteristics, and may be used for both imaging and therapy. Rhenium-188 has a 2110-keV beta emission, complemented by a 155-keV gamma emission, enabling imaging during therapy, although it has a short half-life of 17 hr. The potential of rhenium isotopes already has been demonstrated in early studies using bifunctional chelating agents (*58,59*). These two nuclides have potential for use as therapeutic agents and serve to highlight the versatility of use for MET fusion proteins. Metallothionein fusion proteins, using DNA recombinant technology, also may be made for biologically important ligands, permitting imaging for localization and detection as well as for biological function of tumors. Thus, mouse and human MET genes have been fused to genes encoding human growth hormone and somatostatin (*60,61*). The use of multiple MET sites for metal isotope binding may confer advantages over a single site and needs evaluation.

The successful cloning and subsequent expression and purification of a MET-scFv anti-CEA antibody fragment has led to its use in preclinical studies as an imaging agent for human colorectal tumor. This methodology could have wider implications for tumor imaging, in general, and could permit the use of rhenium isotopes as therapeutic agents.

REFERENCES

1. Larson SM. Clinical radioimmunodetection, 1978–1988: overview and suggestions for standardization of clinical trials. *Cancer Res* 1990;50(suppl):892s–898s.
2. Goldenberg DM, Goldenberg H, Sharkey RM, et al. Imaging of colorectal carcinoma with radiolabeled antibodies. *Semin Nucl Med* 1989;19:262–281.
3. Siccardi AG, Buraggi GL, Callegaro L, et al. Immunoscintography of adenocarcinomas by means of radiolabeled F(ab')$_2$ fragments of an anticarcinoembryonic antigen monoclonal antibody: a multicenter study. *Cancer Res* 1989;49:3095–3103.
4. Siccardi AG. Tumor immunoscintography by means of radiolabeled monoclonal antibodies: multicenter studies of the Italian National Research Council–Special Project "Biomedical Engineering." *Cancer Res* 1990;50(suppl):899s–903s.
5. Hnatowich DJ, Griffin TW, Kosciuczyk C, et al. Pharmacokinetics of an indium-111-labeled monoclonal antibody in cancer patients. *J Nucl Med* 1985;26:849–858.
6. Zalutsky MR, Garg PK, Narula AS. Labeling monoclonal antibodies with halogen nuclides. *Acta Radiol Suppl* 1990;374:141–145.
7. Zalutsky RM, Naruda AS. A method for radiohalogenation of proteins resulting in decreased thyroid uptake of radioiodine. *Int Appl Radiat Isot* 1987;38:1051–1057.
8. Srivastava PC, Buchsbaum DJ, Alfred JF, Brubaker PG, Hanna DE, Spicker JK. A new conjugating agent for radio-iodination of proteins: low in vivo deiodination for a radiolabeled antibody in a tumour model. *Biotechniques* 1990;8:556–562.
9. Hiltunen JV. The search for new and improved radiolabeling methods for monoclonal antibodies: a review of different methods. *Acta Oncol* 1993:8:831–839.
10. Goldenberg DM, Goldenberg H, Sharkey RM, et al. Clinical studies of cancer radioimmunodetection with carcinoembryonic antigen monoclonal antibody fragments labeled with ^{123}I or ^{99m}Tc. *Cancer Res* 1990;50(suppl):909s–921s.
11. Behr TM, Becker WS, Klein MW, et al. Diagnostic accuracy and tumour-targeting kinetics of complete versus fragmented ^{99m}Tc-labeled anti-carainoembryonic antigen antibodies: an intraindividual comparison. *Cancer Res* 1995;55(suppl):5786s–5793s.
12. Pinsky CM, Goldenberg DM, Wlodkowski TJ, Sasso NL, Mojsiak JZ, Hansen HJ. Detection of occult metastases of colorectal cancer by use of anti-CEA Fab' fragments labeled with technetium-99m. *J Nucl Med* 1991;32:1052–1059.
13. Baxter LT, Jain RK. Transport of fluid and macromolecules in tumors. IV. A microscopic model of the perivascular distribution. *Microvasc Res* 1991;41:252–272.
14. Jain RK, Baxter LT. Mechanisims of heterogeneous distribution of monoclonal antibodies and other macromolecules in tumours: significance of elevated interstitial pressure. *Cancer Res* 1988;48:7022–7032.
15. Fujimori K, Covell DG, Fletcher JE, Weinstein JN. A modeling analysis of monoclonal antibody percolation through tumors: a binding site barrier. *J Nucl Med* 1990;32: 1191–1198.
16. Yokota T, Milenic DE, Whitlow M, Schlom J. Rapid tumor penetration of a single-chain Fv and comparison with other immunoglobulin forms. *Cancer Res* 1992;52:3402–3408.
17. Chester KA, Begent RH, Robson L, et al. A new way to generate clinically useful antibodies. *Lancet* 1994;343:455–456.
18. Kagi JHR, Kojima Y. Chemistry and biochemistry of metallothionein. *Experientia* 1987;52:25–61.
19. Gill SC, Von Hippel PH. Calculation of protein extinction coefficients from amino acid sequence data. *Anal Biochem* 1989;182:319–326.
20. Tom BH, Rutzkyk LP, Jakstys MM, Oyasu R, Kaye CI, Kahan BD. Human colonic adenocarcinoma cells. I. Establishment and description of a new line. *In Vitro* 1976;12:180–191.
21. Abraham R, Buxbaum S, Link J, Smith R, Venti C, Darsley M. Screening and kinetic analysis of recombinant anti-CEA antibody fragments. *J Immunol Methods* 1995;183: 119–125.
22. Tjandra JJ, Pietersz GA, Teh JG, et al. Phase I clinical trial of drug-monoclonal antibody conjugates in patients with advanced colorectal carcinoma: a preliminary report [published erratum appears in *Surgery* 1990;107:261]. *Surgery* 1989;106:533–545.
23. Wong DW, Mishkin F, Lee T. A rapid chemical method of labeling human plasma proteins with 99m-pertechnetate at pH 7.4. *Int J Appl Radiat Isot* 1978;29:251–253.
24. Rhodes BA, Zamora PO, Newell KD, et al. Technetium-99m labeling of murine monoclonal antibody fragments. *J Nucl Med* 1986;27:685–693.
25. Chiou RK. The impact of tumor size on the efficacy of monoclonal antibody-targeted radiotherapy: studies using a nude mouse model with human renal cell carcinoma xenografts. *J Urol* 1991;146:232–237.
26. Sahin U, Hartmann F, Senter P, et al. Specific activation of the prodrug mitomycin phosphate by a bispecific anti-CD30/anti-alkaline phosphatase monoclonal antibody. *Cancer Res* 1990;50:6944–6948.
27. Milenic DE, Esteban JM, Colcher D. Comparison of methods for the generation of immunoreactive fragments of a monoclonal antibody (B72.3) reactive with human carcinomas. *J Immunol Methods* 1989;120:71–83.
28. Milenic DE, Yokota T, Filpula DR, et al. Construction, binding properties, metabolism, and tumor targeting of a single-chain Fv derived from the pancarcinoma monoclonal antibody CC49. *Cancer Res* 1991;51:6363–6371.
29. Scatchard G. The attraction of proteins for small molecules and ions. *Ann NY Acad Sci* 1949;51:660–672.
30. Kanellos J, Pietersz GA, McKenzie IFC, Bonnyman J, Baldas J. Coupling of technetium-99m-nitrido group to monoclonal antibody and use of the complexes for the detection of tumors in mice *J Natl Cancer Inst* 1986;77:431–439.
31. Paik CH, Eckelman WC, Reba RC, et al. Transchelation of Tc-99m from low affinity to high affinity sites of antibody. *Nucl Med Biol* 1986;13:359–362.
32. Waalkes MP, Harvey MJ, Klaassen CD. Relative in vitro affinity of hepatic metallothionein for metals. *Toxicol Lett* 1984;20:33–39.
33. George AJT, Jamar F, Tai M-S, et al. Radiometal labeling of recombinant proteins by a genetically engineered minimal chelation site: technetium-99m coordination by single-chain Fv antibody fusion proteins through a C-terminal cysteinyl peptide. *Proc Natl Acad Sci USA* 1995;92:8358–8362.
34. Pietersz GA, Wenjun L, Sutton VR, et al. In vitro and in vivo antitumor activity of a chimeric anti-CD19 antibody. *Cancer Immunol Immunother* 1995;41:53–60.
35. Mount PF, Sutton VR, Li W, et al. Chimeric (mouse/human) anti-colon cancer antibody c30.6 inhibits the growth of human colorectal cancer xenografts in *scid/scid* mice. *Cancer Res* 1994;54:6160–6166.
36. Leung SO, Karacay H, Losman MJ, Griffiths GL, Goldenberg DM, Hansen HJ. Bacterial expression of a kemptide fusion protein facilitates ^{32}P labeling of a humanized, anti-carcinoembryonic antigen (hMN-14) antibody fragment. *Cancer Res* 1995;55(suppl):5968s–5972s.
37. Kortt AA, Malby RL, Caldwell JB, et al. Recombinant anti-sialidase single-chain variable fragment antibody. Characterization, formation of dimer and higher-molecular-mass multimers and the solution of the crystal structure of the single-chain variable fragment/sialidase complex. *Eur J Biochem* 1994;221:151–157.
38. Casey JL, Keep PA, Chester KA, Robson L, Hawkins RE, Begent RH. Purification of bacterially expressed single chain Fv antibodies for clinical applications using metal chelate chromatography. *J Immunol Methods* 1995;179:105–116.
39. Sawyer JR, Tucker PW, Blattner FR. Metal-binding chimeric antibodies expressed in *Escherichia coli*. *Proc Natl Acad Sci USA* 1992;89:9754–9758.
40. Virzi F, Winnard P Jr, Fogarasi M, et al. Recombinant metallothionein-conjugated streptavidin labeled with Re-188 and Tc-99m. *Bioconjugate Chem* 1995;6:139–144.
41. Hnatowich DJ, Mardirossian G, Rusckowski M, Fogarasi M, Virzi F, Winnard P Jr. Directly and indirectly technetium-99m-labeled antibodies: a comparison of in vitro and animal in vivo properties. *J Nucl Med* 1993;34:109–119.
42. Lamki LM, Zukiwski AA, Shanken LJ, et al. Radioimaging of melanoma using ^{99m}Tc-labeled Fab fragment reactive with a high molecular weight melanoma antigen. *Cancer Res* 1990;50(suppl):904s–908s.
43. Kosmas C, Snook D, Gooden CS, et al. Development of humoral immune responses against a macrocyclic chelating agent (DOTA) in cancer patients receiving radioimmunoconjugates for imaging and therapy. *Cancer Res* 1992;52:904–911.

44. Reardan DT, Meares CF, Goodwin DA, et.al. Antibodies against metal chelates. *Nature* 1985;316:265–268.
45. Rodwell JD, Alvarez VL, Lee C, et.al. Site-specific covalent modification of monoclonal antibodies: in vitro and in vivo evaluations. *Proc Natl Acad Sci USA* 1986;83:2632–2636.
46. Rhodes BA. Direct labeling of proteins with ^{99m}Tc. *Int J Radiat Appl Instrum B* 1991;18:667–676.
47. Mather SJ, Ellison D. Reduction mediated Tc-99m labeling of monoclonal antibodies. *J Nucl Med* 1990;31:692–697.
48. Zamora PO, Mercer-Smith JA, Marek MJ, Schulte LD, Rhodes BA. Similarity of copper and Tc-99m binding sites in human IgG *Nucl Med Biol* 1992;19:797–802.
49. John E, Thakur ML, Wilder S, Alarddin MM, Epstein AL. Technetium-99m-labeled monoclonal antibodies: influence of technetium-99m binding sites. *J Nucl Med* 1994;35:876–881.
50. Lash LH, Jones DP. Distribution of oxidized and reduced forms of glutathione and cysteine in rat plasma. *Arch Biochim Biophys* 1985;240:583–592.
51. Cooper AJL. Biochemistry of sulfur-containing amino acids. *Annu Rev Biochem* 1983;52:187–222.
52. Griffith OW, Meister A. Glutathione: interorgan translocation, turnover and metabolism. *Proc Natl Acad Sci USA* 1979;76:5606–5610.
53. Sanyal S, Bannerjee S. Cysteine, a chelating moiety for synthesis of technetium-99m radiopharmaceuticals: II. Attempt to synthesize renal tubular radiopharmaceuticals. *Nucl Med Biol* 1990;17:757–762.
54. Hand PH, Kashmiri SV, Schlom J. Potential for recombinant immunoglobulin constructs in the management of carcinoma. *Cancer* 1994;73:1105–1113.
55. Mastrostamatis SG, Papadopoulos MS, Pirmettis IC, et al. Tridentate ligands containing the SNS donor atom set as a novel backbone for the development of technetium brain-imaging agents. *J Med Chem* 1994;37:3212–3218.
56. Behr T, Becker W, Hannappel E, Goldenberg DM, Wolf F. Targeting of liver metastases of colorectal cancer with IgG, F(ab')$_2$, and Fab' anti-carcinoembryonic antigen antibodies labeled with ^{99m}Tc: the role of metabolism and kinetics. *Cancer Res* 1995;55(suppl):5777s–5785s.
57. Burchiel SW, Hadjian RA, Hladik WB, et al. Pharmacokinetic evaluation of technetium-99-metallothionein-conjugated mouse monoclonal antibody B72.3 in rhesus monkeys. *J Nucl Med* 1989;30:1351–1357.
58. Beaumier PC, Venkatesan P, Vanderheyden JL, et al. Re-186 radioimmunotherapy of small cell lung carcinoma xenografts in nude mice. *Cancer Res* 1991;57:676–681.
59. Breitz HB, Weiden PL, Vanderheyden JL, et al. Clinical experience with rhenium-186-labeled monoclonal antibodies for radioimmunotherapy: results of Phase I trials. *J Nucl Med* 1992;33:1099–1109.
60. Palmiter RD, Norstedt G, Gelinas RE, et al. Metallothionein-human growth hormone fusion genes stimulate growth of mice. *Science* 1983;222:809–814.
61. Low MJ, Hammer RE, Goodman RH, et al. Tissue-specific posttransitional processing of pre-somatostatin encoded by a metallothionein-somatostatin fusion gene in transgenic mice. *Cell* 1985;41:211–219.

Labeling Peptides with Technetium-99m Using a Bifunctional Chelator of a N-Hydroxysuccinimide Ester of Mercaptoacetyltriglycine

D.J. Hnatowich, T. Qu, F. Chang, A.C. Ley, R.C. Ladner and M. Rusckowski
Department of Nuclear Medicine, University of Massachusetts Medical Center, Worcester; and Dyax Corporation, Cambridge, Massachusetts

A modified mercaptoacetyltriglycine (MAG3) chelator, which has acetyl S-protection and which is derivitized with N-hydroxysuccinimide (NHS) ester for conjugation, has been used to radiolabel four small (~6- to 7-kDa) peptides, bovine pancreatic trypsin inhibitor, epidermal growth factor, human neutrophil elastase inhibitor and plasmin inhibitor, with ^{99m}Tc. **Methods:** Each peptide was specifically labeled at the MAG3 chelation sites at ambient temperature and neutral pH. Specific activities of 100–150 mCi/mg were achieved at labeling efficiencies of about 50%, but specific activities of 3500 mCi/μmol could be attained. **Results:** By a variety of assays, protein activity was unimpaired by the conjugation and labeling for two of the four peptides. The activities for plasmin of the plasmin inhibitor and bovine pancreatic trypsin inhibitor were reduced by conjugation, presumably because of a sensitive lysine residue in the structure of each of these two peptides. Multiple peaks were present in the high-performance liquid chromatography radiochromatograms, especially of human neutrophil elastase inhibitor; however, most peaks could be shown to be labeled active peptide. Stability during cysteine challenge at modest cysteine-to-peptide molar ratios and during incubation in serum was observed in each case. Large differences among the labeled peptides were apparent in the 3-hr biodistributions of ^{99m}Tc in normal mice. **Conclusion:** The use of NHS-S-acetyl-MAG3 may be a convenient method of radiolabeling peptides with ^{99m}Tc.

Key Words: peptides; MAG3; technetium-99m

J Nucl Med 1998; 39:56–64

The development of labeled small peptides as radiopharmaceuticals has lately become a minor growth industry, driven, in part, by the success of radiolabeled octeotride in localizing somatostatin receptors (*1*). The list of peptides currently being investigated as potential radiopharmaceuticals for imaging is long (*2*) and growing (*3,4*).

Peptides have been radiolabeled with the radioisotopes of iodine (^{123}I, ^{125}I and ^{131}I), ^{111}In, ^{99m}Tc and other isotopes (*5*). Among those radionuclides that are suitable for single-photon scintigraphy, ^{99m}Tc is considered the superior isotope for most imaging applications. The superiority of ^{99m}Tc as an imaging label for peptides also is predicted because its short (6-hr) physical half-life is an appropriate match with the pharmacokinetics of these molecules, in particular, their rapid rate of whole-body clearance (*5*).

Various and diverse strategies have been described for the labeling of peptides with ^{99m}Tc. For example, under certain circumstances, they may be radiolabeled directly without the prior attachment of an exogenous chelating group. Labeling in this manner usually accompanies the disruption of disulfide bridges within the molecule (*6*). These direct methods of labeling, therefore, will be successful only to the extent that this disruption is not harmful to biological properties, a consequence that may be viewed as unlikely in the case of small peptides, as compared to larger polypeptides or proteins. Another direct and more elegant method of labeling relies on the chelating ability of amino acids that are present in the native peptides or are added during synthesis (*7*). For example, the addition, through genetic engineering, of a Gly-Gly-Gly-Cys tetrapeptide on the C terminus of a peptide will provide a chelating site (*8*). This approach has the advantage of site direction of the chelator, but it cannot be applied to the labeling of preformed peptides.

Most investigators have preferred to prepare ^{99m}Tc-labeled peptides by the conventional use of bifunctional chelators, that is, chelating molecules with functional groups that permit their covalent conjugation to the peptide. One such bifunctional

Received Aug. 5, 1996; revision accepted Mar. 18, 1997.
For correspondence or reprints contact: D.J. Hnatowich, PhD, Department of Nuclear Medicine, University of Massachusetts Medical Center, Worcester, MA 01655.